Macromolecules
PERSPECTIVE

Macromolecules **2010**, *43*, 9217–9226 **9217**
DOI: 10.1021/ma101661p

Bioinspired Polymeric Nanocomposites

David A. Stone and LaShanda T. J. Korley*

Department of Macromolecular Science and Engineering, Case Western Reserve University, Cleveland, Ohio 44106, United States

Received July 23, 2010; Revised Manuscript Received September 16, 2010

ABSTRACT: Nature employs several strategies in fabricating high-performance materials from which scientists can garner important lessons for producing synthetic materials with enhanced properties. When the mechanical properties of a single-phase system are insufficient for an application, composite materials offer an important strategy to impart increased strength and toughness. By introducing nanoscale filler components, greater enhancement in mechanical function compared to traditional macro- and microscale fillers is possible due to the greater surface area and lower percolation thresholds stemming from the higher aspect ratios of the nanoscale fillers. In this Perspective, we will discuss polymer nanocomposites drawing from the lessons of wood (network of preformed, high-modulus cellulose nanorods), spider silk (self-assembly of ordered domains), and tendon (hierarchical ordering).

Introduction

Bioinspiration has been defined as "when biological concepts, mechanisms, functions, and design features are abstracted as a starting point on the road to new synthetic materials and devices with advanced structures and functions".[1] Direct imitation is often not the goal of bioinspired materials, but instead, creative use of design motifs found in nature are employed to fabricate novel materials.[2] Nature employs several strategies in fabricating high-performance materials from which scientists can glean important lessons. One of the most straightforward and abundant natural composites is wood, whose cell walls are comprised of cellulose fibers embedded in a matrix of lignin.[3] The strength and elasticity of the wood are largely governed by the ordering of the cellulose fibers in the protein matrix.[4] Spider silk has also been long studied for its blend of high strength and flexibility.[5] Its mechanical properties come from crystalline domains tethered together by amorphous regions.[6,7] Tendon is comprised of ordered collagen bundles tied together by a matrix of proteoglycans.[8] Because of the hierarchical ordering of the tendon, the overall strain of the tendon is always larger than the strain exhibited in the individual fibrils.[9]

Using the previous examples, several important lessons are evident from the design and function of the natural composite materials. While each of the previously mentioned natural systems involves many factors to obtain their unique properties, an illustrative property of each system will be discussed as inspiration for man-made composite materials. For example, wood demonstrates the importance having a well-dispersed network of high-strength rods in a softer matrix to impart increased strength.[3] Furthermore, by using components with complementary strengths (a matrix with high compressive strength and a filler with high tensile strength, for example), a synergistic net effect can be attained.[10] For spider silk, the role of self-assembly in processing and material function is shown. Spiders store the silk-forming proteins in a β-sheet-deficient conformation, allowing the proteins to maintain solubility and facilitate the spinning process. During spinning, a morphological transition from a β-sheet-deficient to β-sheet-rich material occurs, providing the unique combination of strength, flexibility, and toughness observed in spider silk.[5] Finally, hierarchical ordering within a composite, such as a tendon, can contribute to interesting mechanical properties.[11] With ordering across multiple scales, stress relief events due to the reorganization of individual components can be an avenue toward increased toughness.

While polymeric materials give rise to a wide array of bulk properties depending upon their molecular composition and architecture,[12] these material properties can be insufficient for some demanding technologies, such as high-strength and low-weight materials needed for the wings on airplanes. Various high-performance polymers have been developed by incorporating rigid or associative segments into the polymer backbone, but a balance between strength and processability must be found for practical applications. In order to access material properties otherwise unobtainable via pure polymers while maintaining processability, additives and fillers are often introduced to a polymer matrix to generate a composite material.[13,14] A composite is generally defined as a material comprised of two or more constituents that have significantly different mechanical properties and that remain separate and distinct within the final structure.[15]

To be considered a nanocomposite, the size of the filler component must be on the nanoscale.[16,17] Early additives to be exploited in polymer composites, such as glass fibers (diameter $\sim 10-30$ μm), were generally microscopic in scale. While enhanced mechanical properties were achieved with these materials, the enhancement per weight of filler was limited because of the low surface area to volume ratio. Recent focus has shifted to the use of nanoscale fillers in lieu of the traditional microscopic fillers in order to expand the potential range of composite materials even further.[14,18] Nanoscale fillers typically have much higher aspect ratios that lead to greater surface area per mass and lower percolation thresholds which enable mechanical enhancement at lower filler contents than with traditional fillers.[19] Because less filler material is needed, lighter and more cost-effective materials have been produced and used by the automotive, aerospace, and construction industries.[20] To push the capabilities of nanocomposites to the next level, researchers are utilizing lessons from nature to design the next generation of materials.

*Corresponding author: e-mail lashanda.korley@case.edu, Ph (216)-368-1421, Fax (216)368-4202.

Published on Web 10/04/2010

Polymeric composite materials are typically classified as either hybrid, both organic and inorganic components, or wholly organic. Hybrid polymer composites have been reviewed in several other articles.[21−23] This Perspective focuses on polymer nanocomposites comprised purely of organic components. While polymeric composites have been developed to enhance optical,[24−26] electrical,[27−29] and a host of other properties,[30−32] we are focusing primarily on enhancement and tailoring of mechanical behavior. Although most synthetic nanocomposite materials lack the complexity of natural composites, researchers are actively trying to incorporate these strategies to fabricate novel, multifunctional composite materials. In this paper, we will discuss polymer nanocomposites drawing from the lessons of wood (network of preformed, high-modulus cellulose nanorods), spider silk (self-assembly of ordered domains), and tendon (hierarchical ordering). Specifically, we will cover (i) preformed rods from renewable resources as filler materials, (ii) self-assembled small molecules, and (iii) fibers generated by electrospinning (Figure 1). We will conclude with remarks regarding the future direction of polymer nanocomposite research.

David A. Stone is currently a Research Associate in the Macromolecular Science and Engineering department at Case Western Reserve University under Prof. LaShanda Korley and Prof. Gary Wnek. He received his B.S. in Chemistry from the University of Wisconsin—Madison in 2003. In 2008, he received his Ph.D. in Chemistry from Northwestern University under the guidance of Prof. Samuel Stupp where he investigated the self-assembly of conjugated small molecules for electronic applications.

LaShanda T. James Korley is the Nord Distinguished Assistant Professor of Macromolecular Science and Engineering at Case Western Reserve University. Korley received B.S. degrees in Chemistry and Engineering from Clark Atlanta University and a B.S. in Chemical Engineering from the Georgia Institute of Technology. Under the direction of Professors Paula T. Hammond and Gareth H. McKinley, she received her Ph.D. in Chemical Engineering/Program in Polymer Science and Technology from the Massachusetts Institute of Technology. Prior to joining the faculty of Case Western Reserve University in 2007, LaShanda was postdoctoral fellow at Cornell University in the School of Chemical and Biomolecular Engineering. Prof. Korley recently received a National Science Foundation CAREER Award and 3M Nontenured Faculty Award. Her research program focuses on bioinspired approaches to material toughening, confinement-induced assembly of polymeric nanocomposites, and strategies for tailored therapeutic delivery.

Lessons from Wood: Network of Preformed Cellulose Nanorods

Polymer composite materials based on preformed rods are among the earliest developed. Nanocomposites based upon carbon nanotubes and inorganic materials (such as clay and silica particles) have shown an increase in mechanical properties, especially the heat distortion temperature, compared to the neat polymer.[33,34] More recently, there has been a push to develop composite materials from renewable and biodegradable resources due to environmental concerns. To move away from materials derived from nonrenewable resources, fibers comprised of cellulose, which is isolated from renewable and abundant materials, have become the focus of much investigation.[35] The fibers, which have high strength due to their crystalline structure, can be isolated from a wide variety of sources, including wood, cotton, algae, bacteria, and sea tunicates. These cellulose fibers typically have aspect ratios varying between 10 and 100 and diameters ranging from 4 to 20 nm, depending on the cellulose source.[36] The high elastic moduli (100−150 GPa) of cellulose fibers makes them an excellent reinforcing component in polymer nanocomposites.[37,38] In this section, we will highlight examples that demonstrate the state of the field. For a comprehensive study on the subject, the following reviews are recommended.[39−42]

One area where cellulose nanofiber composite materials are of extreme interest is in optically transparent applications. When the individual components of a composite material are one-tenth the wavelength of light, these composites are typically free of scattering. Yano et al. investigated various resins (including epoxy, acrylic, and phenol−formaldehyde) at high loadings of cellulose fibers derived from bacteria (Figure 2a).[43] It was found that at 60−70 wt % loading of cellulose fibers in epoxy resin up to 80% transmission of the incident light was achieved, as shown in Figure 2b. The transmission loss attributed to the nanofiber network was found to be less than 10% even though refractive indices of the two components are mismatched. Coupled with high transparency, the nanocomposite films were found to exhibit significantly higher mechanical strength and lower thermal expansion coefficients. The Young's modulus of the composite film was 20−21 MPa, while the tensile strength reached values near 325 MPa.

As another example, Tang and Weder recently studied epoxy resins reinforced with cellulose nanofibers isolated from sea tunicates and cotton.[44] While nanofibers isolated from sea tunicates have a higher aspect ratio than cotton-derived fibers, cotton is a more readily available source material. The authors developed a simplified composite fabrication technique using solvent exchange instead of lyophilization and redispersion of the cellulose nanofibers that is commonly employed to fabricate cellulose nanocomposite films. This strategy is important because lyophilization is typically a limiting step in terms of time, energy, and cost for the film production process. Using this simplified approach, films with a well-dispersed percolating network of nanofibers were fabricated. While the inclusion of cellulose nanofibers was found to only moderately improve the mechanical properties below the glass transition temperature (T_g) of the epoxy matrix, once above the T_g of the matrix, the tensile storage modulus was found to significantly increase from ~16 MPa for

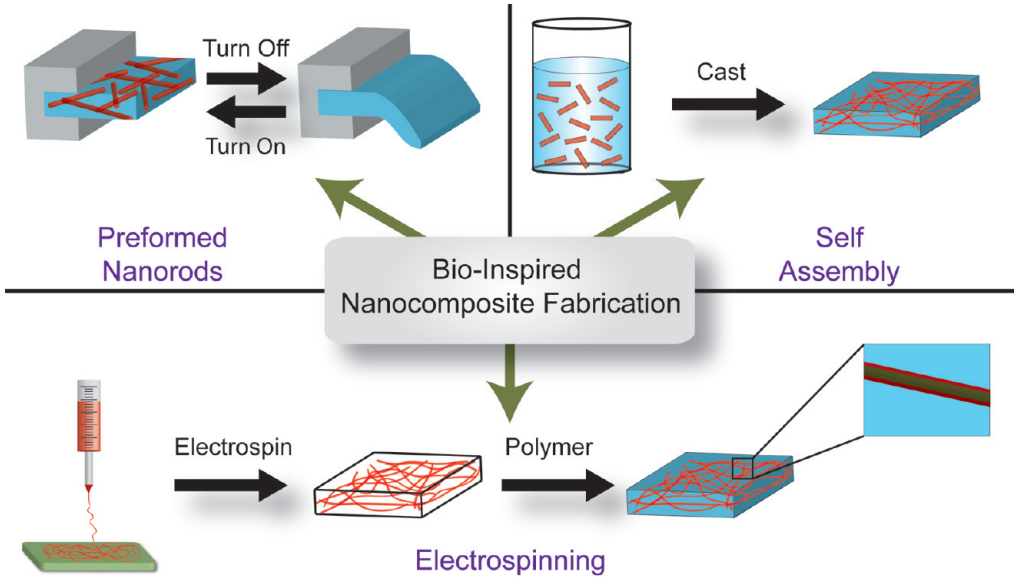

Figure 1. Schematic representation of fabrication methods for bioinspired polymer nanocomposites.

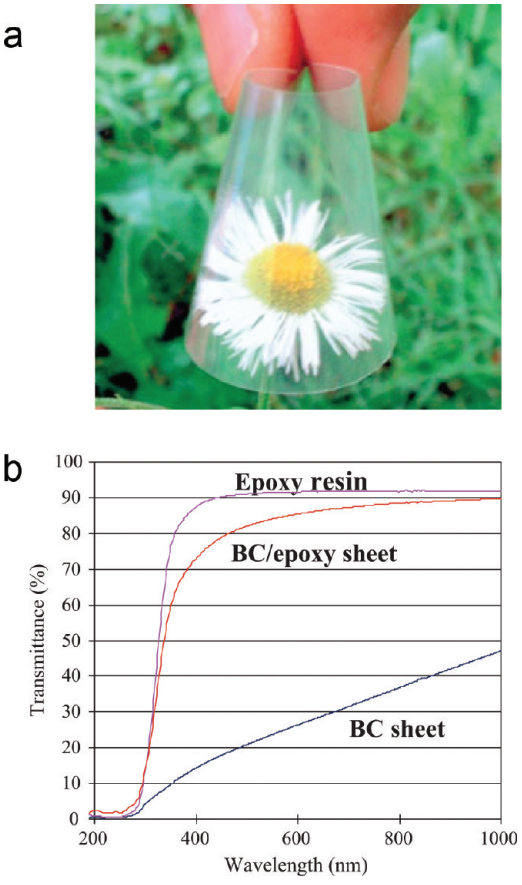

Figure 2. (a) Flexibility of a 65 μm thick bacterial cellulose sheet with acrylic resin A600 (60 wt % fiber content). (b) Light transmittance of a 65 μm thick cellulose/epoxy−resin sheet (65 wt % fiber content), a bacterial cellulose (BC) sheet, and an epoxy−resin sheet. Reproduced with permission from ref 43. Copyright 2005 Wiley-VCH Verlag GmbH & Co. KGaA.

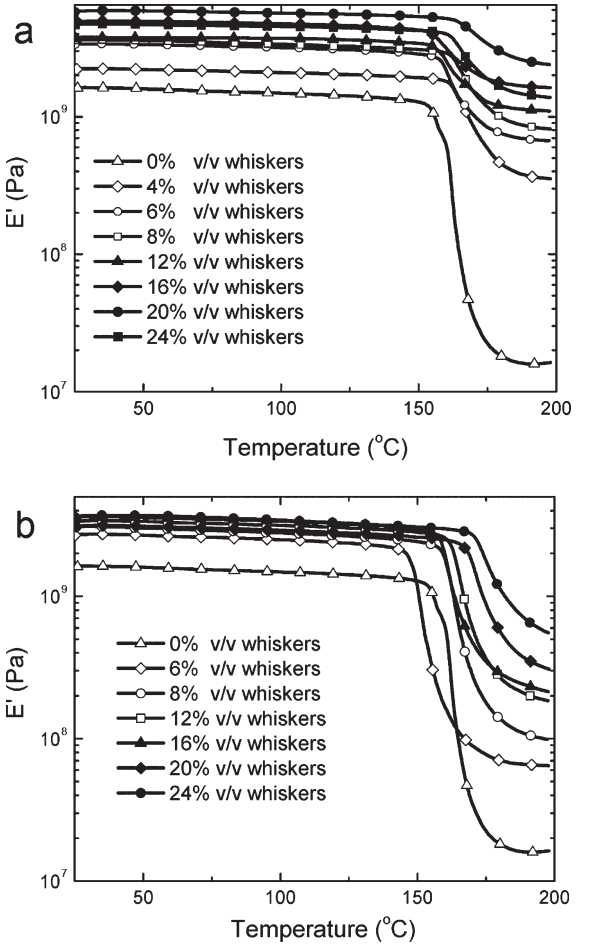

Figure 3. Tensile storage moduli (E') of (a) tunicate whisker/epoxy and (b) cotton whisker/epoxy nanocomposites made by redispersion of acetone/whisker gels in DMF. The nanocomposites contain between 0 and 24% v/v tunicate whiskers. Adapted and reprinted with permission from ref 44.

the matrix polymer to ~1.6 GPa for sea tunicate (Figure 3a) composites and ~215 MPa for cotton composites (Figure 3b).

The rising interest in cellulose-based polymer nanocomposites necessitates a detailed understanding of the interactions between the filler and the matrix that give rise to enhanced properties. Raman spectroscopy has emerged as a powerful tool for evaluating the stress transfer from polymer matrix to the cellulose nanofibers.[38,45,46] Eichhorn et al. have used this technique to

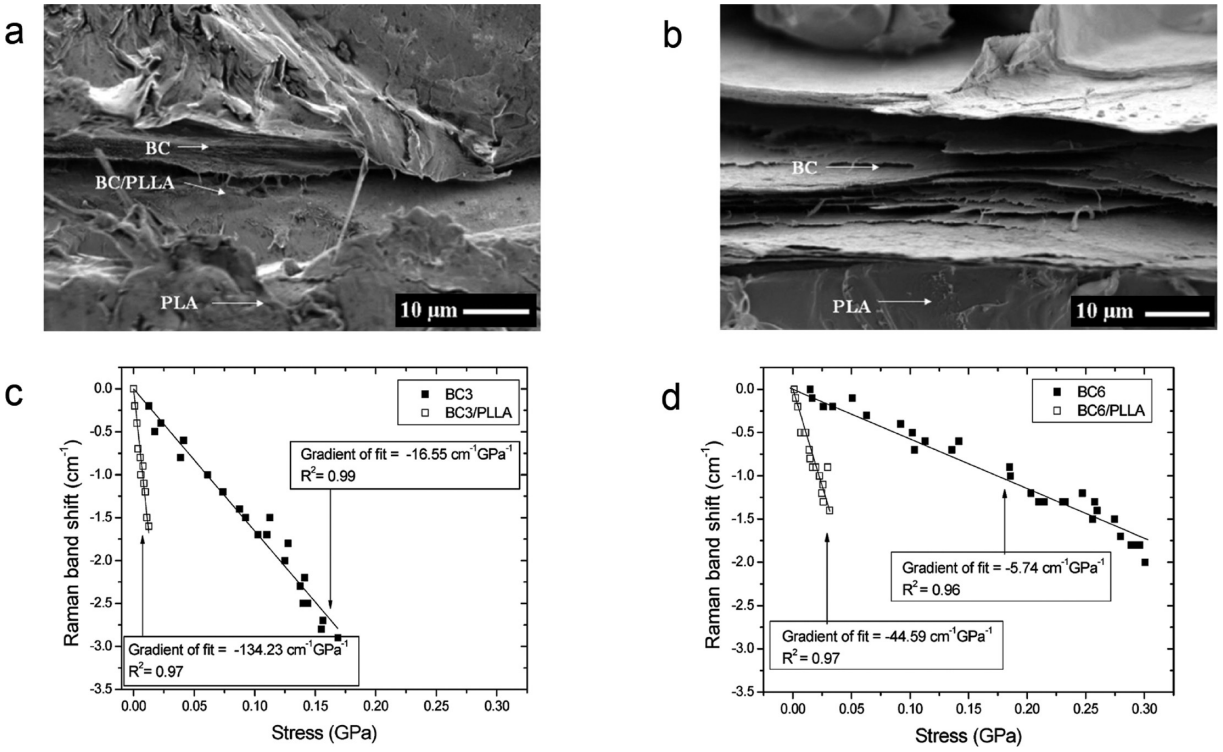

Figure 4. Typical scanning electron microscope (SEM) images of fractured surfaces of (a) a bacterial cellulose network cultured for 3 days/PLLA composite and (b) a bacterial cellulose network cultured for a 6 days/PLLA composite. Typical shifts in the peak position of the Raman band initially located at 1095 cm^{-1} for (c) a bacterial cellulose network cultured for 3 days (BC3) with respect to stress and a bacterial cellulose network cultured for 3 days/PLLA composite (BC3/PLLA) comprising this network with respect to stress and (d) for a bacterial cellulose network cultured for 6 days (BC6) and a bacterial cellulose network cultured for 6 days/PLLA composite (BC6/PLLA) with respect to stress. Reprinted with permission from ref 47.

study stress transfer efficiency between composite films of poly(L-lactic acid) (PLLA) and bacteria-derived cellulose nanofibers cultured for either 3 (BC3) or 6 days (BC6), which primarily impacts the total surface area of the filler, as shown in Figure 4.[47] The composites fabricated from bacterial cellulose cultured for 3 days were found to have ~15 times the surface area of the nanocomposites fabricated from bacterial cellulose cultured for 6 days as measured by nitrogen adsorption. The Young's modulus and stress-at-failure were found to increase for both PLLA nanocomposites compared to neat PLLA. While the overall increase in the modulus and failure stress was higher for the BC6 nanocomposites compared to the BC3 nanocomposites, the specific Young's modulus (divided by density) was similar. The BC3 nanocomposite was found to have an increased interaction with PLLA matrix, which was attributed to the significantly increased surface area compared to the BC6 nanocomposite. This investigation highlights the importance of understanding and controlling matrix−filler interactions to develop polymeric nanocomposites with similar or superior mechanical properties while using limited material.

Beyond nanocomposite films, cellulose nanofibers have also been used to increase the mechanical properties of high-porosity foams.[48−50] High-porosity foams typically exhibit poor strength and are susceptible to water degradation due their very low density. Berglund et al. incorporated up to 40 wt % of microfibrillated cellulose into an amylopectin foam before the porous cell structure was disrupted.[51] With the inclusion of cellulose nanofibers into the foam structure, significant improvements in modulus, yield strength, and resistance to aqueous degradation were reported. Above 40 wt % loading of cellulose nanofibers, a reduction in mechanical behavior was observed due to the loss of the open cell structure in the foam nanocomposite.

Another emerging field in polymer nanocomposite research is the fabrication of stimuli-responsive or "smart" materials. One recent and promising example of an all organic, stimuli-responsive polymer nanocomposite that closely mimics the adaptability and structure of the sea cucumber dermis (Figure 5a, b) was reported by Capadona et al.[52] Nanocomposite materials made from a rubbery matrix and cellulose nanofibers isolated from tunicates were fabricated by solution casting followed by compression molding. When exposed to a chemical stimulus, in this case water, the interactions between the rigid cellulose nanofibers of the filler are minimized (Figure 5c). Upon the weakening of the support matrix, the tensile modulus was found to reversibly decrease by a factor of 40 when ethylene oxide−epichlorohydrin 1:1 copolymer (EO−EPI) was used as the matrix (Figure 5d). The modulus differential was even more dramatic, up to several orders of magnitude, when filler softening is coupled with a thermal transition (T_g) of the polymer matrix as shown with a poly(vinyl acetate) (PVAC) matrix (Figure 5e). Similar results have been achieved using cotton, a much more readily available and industrially relevant material, as the source of cellulose nanofibers.[53]

Using a construction inspired by natural wood, stiff filler rods in a soft matrix, stronger polymeric materials have been produced. Cellulose nanofibers have been shown to be a versatile and robust natural filler material for use in a multitude of applications. Mechanically dynamic materials using cellulose nanofibers have been realized by understanding and controlling the filler−filler and filler−matrix interactions. The possibility of multifunctional or multistimuli responsive nanocomposite materials exists with the introduction of additional switching segments to control and tailor filler interactions.

Lessons from Spider Silk: Self-Assembly of Ordered Domains

Over the past few decades, the self-assembly of molecules into supramolecular structures has been at the heart of intense research efforts.[54,55] Using organization strategies inspired by

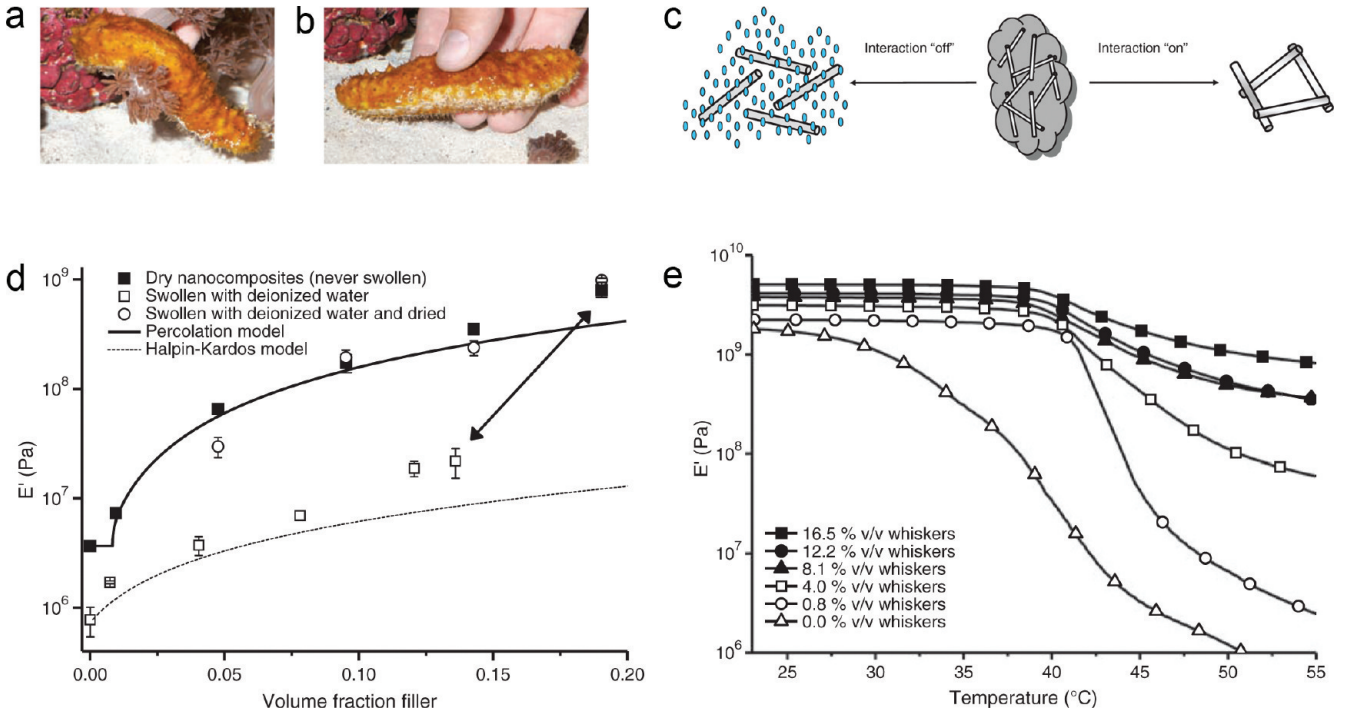

Figure 5. Pictures of a sea cucumber in relaxed (a) and stiffened (b) state demonstrating the firming of dermal tissue in the vicinity of the contacted area. (c) Schematic representation of the architecture and switching mechanism in the artificial nanocomposites with dynamic mechanical properties. In the "on" state, strong hydrogen bonds between rigid, percolating nanofibers maximize stress transfer and therewith the overall modulus of the nanocomposite. The interactions are switched "off" by the introduction of a chemical regulator that allows for competitive hydrogen bonding. (d) Tensile storage moduli E' of EO−EPI/whisker nanocomposites as a function of volume fraction of cellulose whiskers. The nanocomposites were conditioned by either drying in vacuum, equilibrium swelling in deionized water, or swelling to saturation in deionized water followed by redrying in vacuum. Lines represent values predicted by the percolation and Halpin−Kardos model. The arrow indicates changes in modulus and volume fraction of whiskers resulting from aqueous swelling of one selected sample (19% v/v whiskers). (e) Tensile storage moduli E' of dry films of PVAc/whisker nanocomposites as a function of temperature. The nanocomposites contain between 0 and 16.5% v/v whiskers. Reproduced with permission from ref 52. Copyright 2008 AAAS.

nature, scientists have been able to controllably create assemblies of molecules into an array of ordered and functional architectures.[56,57] Along with the advancement of fields such as organic electronics[58−61] and regenerative medicine,[62,63] self-assembling small molecules have also been of interest as the filler component in polymer nanocomposite materials. Using nature-inspired self-assembly of small molecules into nanostructures as a nanocomposite fabrication strategy, nanocomposite materials with structures reminiscent of spider silk that display improved mechanical properties have been developed.

One of the earliest self-assembling small molecule fillers in polymer nanocomposite materials is dibenzylidene sorbitol (DBS).[64−66] DBS is a butterfly-shaped amphiphile capable of inducing gel formation in various organic liquids and polymer melts by forming a 3D network of nanofibers.[67,68] Spontak et al. studied thermal and mechanical properties of a DBS derivative, 1,3:2,4-di-*p*-methylenebenzylidene (MDBS), in the matrix of a polypropylene copolymer with 3 wt % ethylene.[65] The MDBS nanofibers served as nucleation sites, which induced heterogeneous nucleation of polymer spherulites. At lower concentrations, MDBS served as a clarifying agent, resulting in films with increased transparency and yield strength. At higher concentrations of MDBS, the diameter of the nanorods increased, reducing optical clarity but further improving the ultimate mechanical properties. It was postulated these results indicate that at higher concentrations MDBS acts as a reinforcing agent, but at lower concentrations it behaves as a clarifying or nucleating agent.

The Stupp laboratory developed a class of molecules known as dendron rod−coils (DRC) that self-assemble into nanoribbons approximately 10 nm wide, 2 nm thick, and micrometers long.[69,70] In styrene monomer, the DRCs were found to induce gel formation at concentrations as low at 0.1 wt %.[71] Upon thermal polymerization of the preformed gel, birefringence was found to increase with a maximum at 0.5 wt % of DRC. The observed increase in birefringence was attributed to increased alignment of the polymer chains induced by the DRC nanofibers.[72] The authors also noted that the Charpy impact strength of the polystyrene/DRC nanocomposite with 0.5 wt % DRC was nearly double that of pure polystyrene.[73] It was also revealed that the improved toughness and ductility of the nanocomposites were due to increased stress whitening and craze density in the DRC modified films (Figure 6). The smaller and higher-density crazes in DRC composites resembled those formed in more highly oriented polymers when stressed in tension along their axis of orientation. The filler-induced change of local polymer chain orientation in these DRC-based nanocomposites modified the crazing patterns, enhancing mechanical behavior.

More recently, Bouteiller et al. studied the reinforcement of bitumen via small molecule incorporation.[74] Using readily available aliphatic diacids as the self-assembling nanofiller, a percolated network of micrometer long nanofibers formed upon cooling in bitumen at concentrations as low as 3 wt %.[75] The softening temperature of bitumen was studied to investigate the reinforcement of the matrix, revealing that, with as low as 3 wt % of diacid incorporated into the composite, the softening temperature increased by as much as 60 °C (Figure 7), suggesting mechanical reinforcement of the bitumen matrix. It was determined that, below room temperature, the elastic modulus is an order of magnitude higher for the nanocomposite material than pure bitumen. Although the room temperature mechanical properties were enhanced with the inclusion of self-assembling diacids, the melt viscosity at typical processing temperatures remained unchanged.

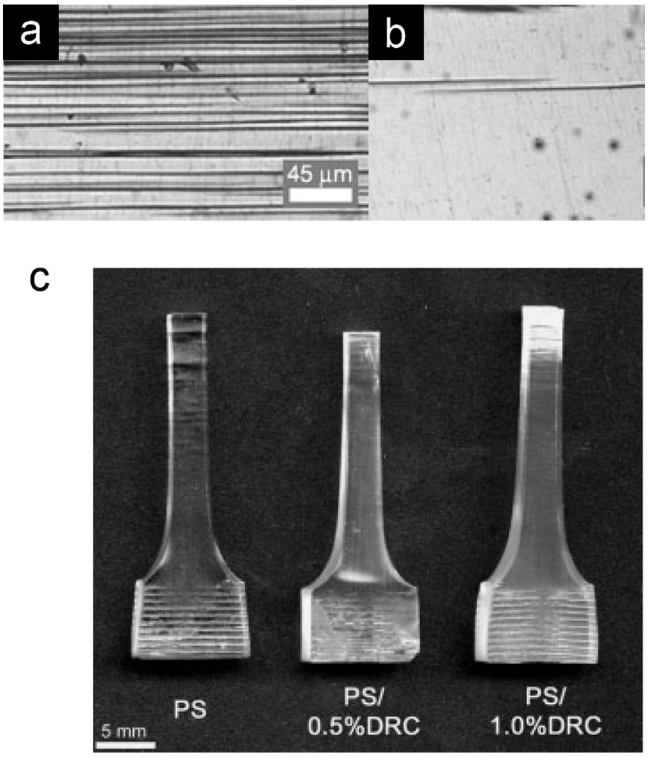

Figure 6. Transmission optical microscopy images of craze microstructure of 250%-prestrained specimens just below the fracture surfaces of (a) PS/0.5 wt % DRC and (b) PS homopolymer. (c) Pictures of 250% prestrained tensile specimens after testing failure in uniaxial tension. Reproduced with permission from ref 73. Copyright 2005 Wiley-VCH Verlag GmbH & Co. KGaA.

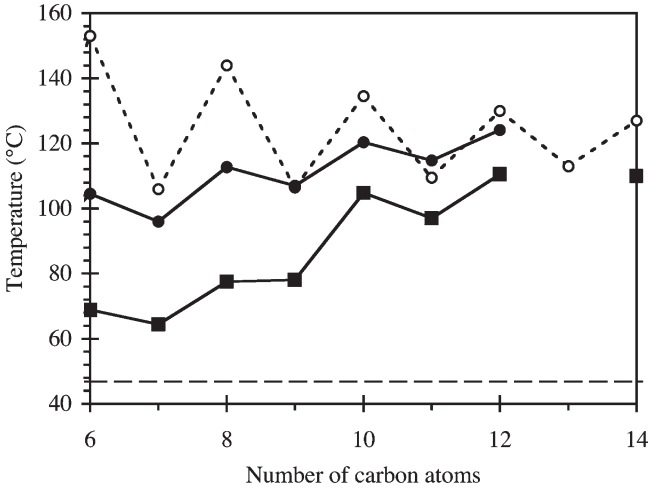

Figure 7. Softening temperature of bitumen with 3% (w/w) diacid (■) vs the number of carbon atoms of the diacids. These values can be compared to the softening temperature of pure bitumen (- - -), the melting temperature (○), and the sublimation temperature (at a pressure of 0.5 Pa) (●) of pure diacids. Reproduced with permission from ref 74.

The interaction between the matrix and filler is crucial for optimal performance in polymer nanocomposite materials. As an example, when segmented polyurethanes are mixed with smectic clay particles, enhancement of the thermomechanical properties occurs only when the clay particles are confined within the hard segment of the polymer.[76] When the clay particles are located in the soft segment, substantial reduction in toughness and extensibility occurs. While most composite materials rely on simple mixing to achieve matrix−filler interaction, using molecular recognition, similar to the "lock-and-key" mechanisms pervasive throughout biological systems, is an underused strategy to impart mechanical enhancement of polymeric systems. Meijer et al. developed a molecular filler designed to be a perfect fit with the corresponding elastomeric polymer shown schematically in Figure 8a.[77,78] They found that mixing up to 7.3 wt % (23 mol %) increased the Young's modulus by over 100% while not influencing the yield strength, tensile strength, and strain at break (Figure 8b−d). At concentrations below 23 mol %, the fillers preferentially associated with the hard segment due to matching hydrogen bonding motifs and molecular size. Above 23 mol %, the filler began to phase separate, forming a secondary hard phase in the composite material. Furthermore, studies have revealed that filler materials with nonmatching or without hydrogen-bonding groups tend to not interact with the polymer hard segments, further underscoring the importance of molecular compatibility needed for optimal properties.[79]

Using self-assembling small molecules offers an important processing advantage over preformed particles or rods by not altering the melt rheology and mimics nature's strategy for spinning spider silk. As previously mentioned, spider silk is stored in a random conformation, allowing the protein to maintain solubility. Once spun, a conformational transformation occurs, yielding the crystalline domains needed for its mechanical integrity. Since the self-assembly of small molecules is often reversible by external stimuli, usually via temperature, only minimal impact on the melt viscosity would be expected upon dissolution of the small molecule additive at low concentrations. After processing and upon cooling, the small molecules can then assemble into a nanofibrillar arrangement, creating the reinforcing filler component. Furthermore, by controlling the crystallinity and size parameters of the self-assembled nanofibers, the mechanical properties of the composites should be able to be controlled.

Lessons from Tendon: Hierarchical Ordering

Although the first patent that described the electrospinning process was filed in 1934,[80] this technique has garnered much attention over the past couple of decades because of its ability to create nanofibers from a wide array of polymers for applications ranging from cell scaffolds to filtration membranes and electronic devices to drug delivery vehicles.[81−84] In electrospinning, fibers are generated by applying an electric field between a polymer solution and a grounded collector. When the electrostatic force overcomes the surface tension of the polymer solution, a stable jet or "Taylor cone" can be formed. As the jet travels toward the collector, it is constantly subjected to a stretching movement producing nanofibers of tunable diameter.[85] Nanofibers fabricated via electrospinning have also been used as the filler component in polymer nanocomposite materials.[86] These electrospun nanofibers can be oriented into ordered arrays, providing a pathway to fabricate hierarchically organized composites with an arrangement inspired by the fiber packing observed in tendon.

The first examples of nanocomposite materials fabricated from electrospun nanofiber mats were independently reported by Bergshoef and Vancso[87] and Kim and Reneker[88] in 1999. Bergshoef and Vancso studied nanocomposite films of uniform, electrospun nylon-4,6 (30−200 nm diameter) in an epoxide matrix. At only ~4 wt % loading of nanofibers, the Young's modulus and fracture stress were found to significantly increase, while the fracture strain significantly decreased. Kim and Reneker studied both epoxide and rubber matrices reinforced

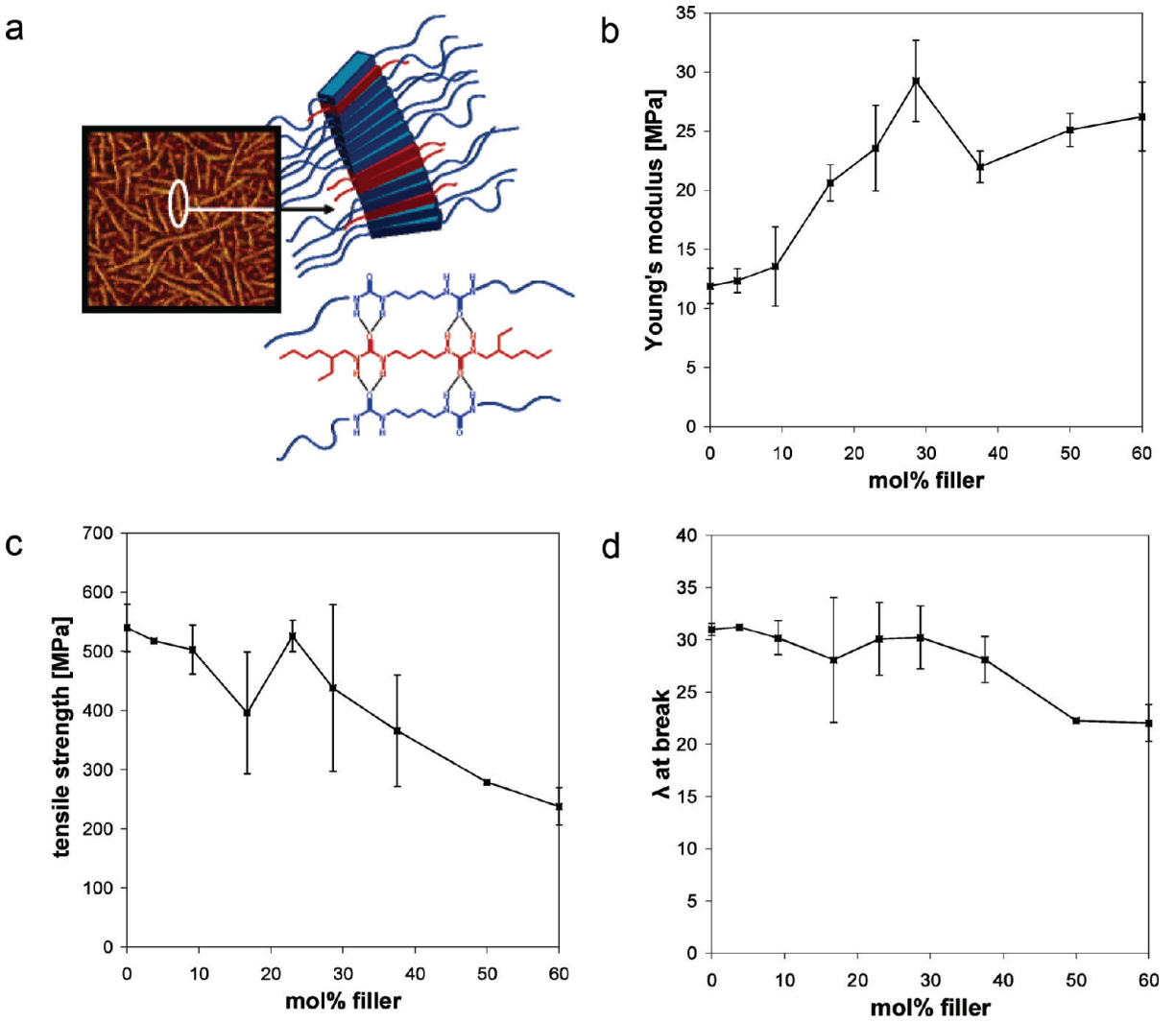

Figure 8. (a) Proposed modular approach: the supramolecular filler (red) is incorporated into the polymer hard domains (blue) via bifurcated hydrogen bonds. Young's modulus (b), tensile strength (c), and λ at break (d) of films containing increasing amounts of filler. Data derived from true $\sigma-\lambda$ curves. Reproduced with permission from ref 77.

with fibrous mats of poly(benzimidazole) (PBI). When incorporated into epoxy resins, the Young's modulus, fracture toughness, and the fracture energy were found to increase with increasing content of PBI fibers. Furthermore, when compared against composite films containing a commercial PBI fiber filler, a more significant enhancement in mechanical properties was reported via incorporation of the electrospun PBI fibers due to the increased surface area of the electrospun fibers. In a rubber matrix, the Young's modulus of the PBI nanofiber-reinforced composite was 10 times higher than the neat rubber and significantly higher than carbon black reinforced rubber composite materials.

Tang and Liu investigated poly(vinyl alcohol) (PVA) films reinforced with a cellulose nanofiber mat electrospun from an acetone/*N,N*-dimethylacetamide solution with fibers ranging between 100 and 900 nm.[89] Complete hydrolysis of the cellulose mat was achieved via treatment with a base, which facilitated impregnation with hydrophilic PVA to produce highly transparent films. The cellulose acetate fibers are relatively hydrophobic, but upon hydrolysis, the hydrophilic alcohol groups were able to hydrogen bond with the PVA, creating a uniform composite film. These PVA/electrospun cellulose nanofiber films with loadings up to 40 wt % transmitted 75% of incident light (Figure 9a). At high cellulose nanofiber content, the PVA composite exhibited an increase in mechanical strength by 50% and Young's modulus by more than 600% (Figure 9b).

Another area in which polymeric nanocomposite containing electrospun fillers have found application is in shape memory elastomeric materials. Luo and Mather created shape memory elastomeric composites from electrospun mats of poly(ε-caprolactone) (PCL) and a silicone rubber (Sylgard 184), as shown in Figure 10.[90] Thermal characterization revealed that the composite film has three distinct transitions attributed to the glass transition of Sylgard 184 (T_g = −114.4 °C), the glass transition of PCL (T_g = −49.5 °C), and the melting transition of PCL (T_g = 60.6 °C). Shape memory was imparted to the elastomeric nanocomposite through the melting of the semicrystalline PCL fibers. The Sylgard composite showed a sharp recovery centered at 60 °C, corresponding to the melting temperature of the PCL fibers and exhibited almost complete shape fixing and recovery.

By controlling the hierarchical ordering within electrospun composites, tunable and responsive mechanical properties are achievable. For example, exploitation of the crystalline structure within the electrospun fibers makes possible shape memory behavior. Electrospinning is a facile and readily adaptable processing technique, which affords a unique strategy for the development of ordered, nanofiber arrays. By using well-aligned

nanofibers, mechanically anisotropic materials are also feasible. Using core−shell nanofibers produced by coaxial electrospinning, the potential to fabricate composites with a hierarchical structure reminiscent of the organization in tendon exists.

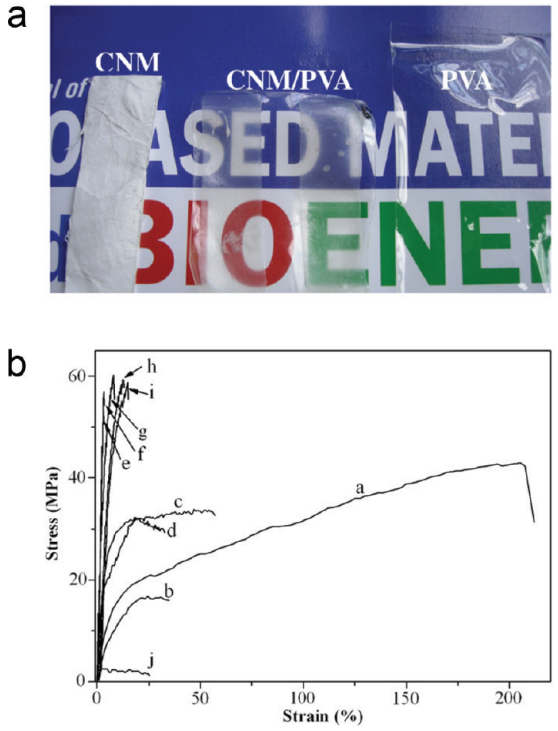

Figure 9. (a) Appearance of films. Cellulose nanofibrous mat (CNM)/PVA composite film contains 40 wt % CNM. (b) Stress−strain curves of CNM/PVA composite films. Mass content of CNM in the composite films is (a) 0, (b) 4.7, (c) 5.5, (d) 8.4, (e) 23, (f) 24, (g) 40, (h) 50, (i) 60, and (j) 100. Reproduced with permission from ref 89. Copyright 2008 Elsevier.

Conclusion

Nature has employed nanocomposite construction as a versatile strategy for the development of materials with unique physical properties. While synthetic nanocomposite materials have generally lacked the sophistication of their natural counterparts, researchers have used strategies inspired by nature to push the properties of composite materials further. This Perspective has examined three strategies for the development of all-organic polymer nanocomposites: (i) preformed nanorods from renewable resources, (ii) self-assembled small molecules, and (iii) electrospun nanofibers. By fine-tuning these fabrication strategies, researchers have been able to create nanocomposites materials with unique physical properties. Further development of novel filler materials to optimize the filler−matrix interactions, known to be very important in traditional composite materials, should lead to organic nanocomposites with even greater performance. Bioinspired strategies will drive the design of more sophisticated filler materials, influence the manipulation of filler−matrix and filler−filler interactions, and spur innovative processing pathways in the development of multifunctional, mechanically enhanced polymer nanocomposites.

Acknowledgment. The authors thank the National Science Foundation (NSF) (CAREER DMR-0953236 and BRIGE EEC-0824333) and Army contract W911QY-08-C-0142 for support. We also thank Dr. Lorraine Hsu for thoughtful discussions and helpfulness throughout the writing process.

References and Notes

(1) Dujardin, E.; Mann, S. *Adv. Mater.* **2002**, *14* (11), 775–788.
(2) Bruet, B. J. F.; Song, J. H.; Boyce, M. C.; Ortiz, C. *Nature Mater.* **2008**, *7* (9), 748–756.
(3) Fratzl, P.; Weinkamer, R. *Prog. Mater. Sci.* **2007**, *52* (8), 1263–1334.
(4) Gindl, W.; Teischinger, A. *Composites, Part A* **2002**, *33* (12), 1623–1628.
(5) Kenney, J. M.; Knight, D.; Wise, M. J.; Vollrath, F. *Eur. J. Biochem.* **2002**, *269* (16), 4159–4163.

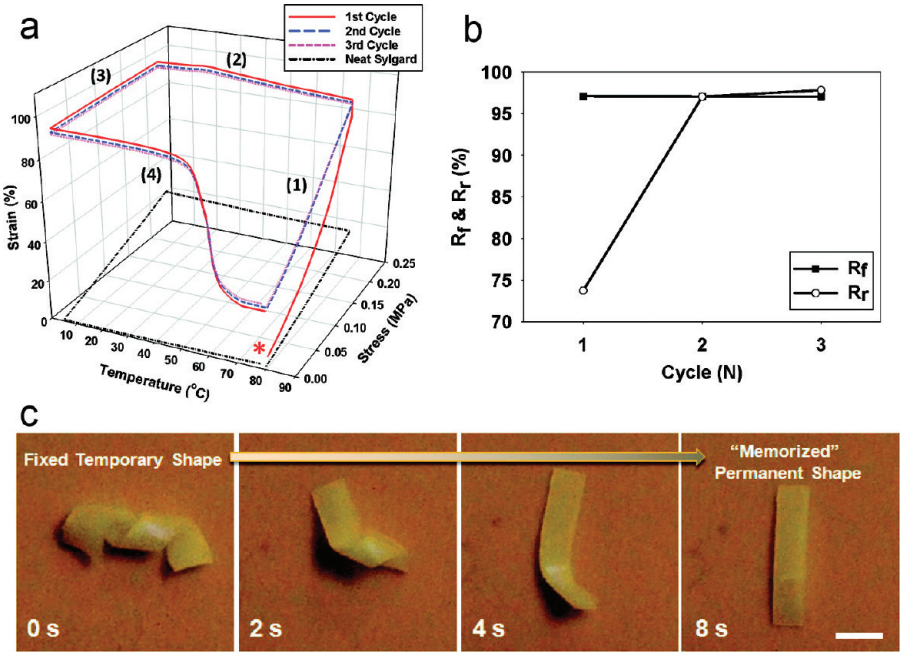

Figure 10. Shape memory properties of Sylgard/PCL SMECs. (a) Stress−temperature−strain plot showing the one-way shape memory (1WSM) cycles of Sylgard/PCL, compared with neat Sylgard (the asterisk indicates the onset point). (b) Fixing ratio (R_f) and recovery ratio (R_r) calculated for three cycles. (c) Photographs of Sylgard/PCL composite showing the recovery from a fixed temporary shape to its "memorized" permanent shape on a temperature-controlled plate at 80 °C (the scale bar represents 5 mm). Reproduced with permission from ref 90.

(6) Gosline, J. M.; Guerette, P. A.; Ortlepp, C. S.; Savage, K. N. *J. Exp. Biol.* **1999**, *202* (23), 3295–3303.
(7) Jin, H. J.; Kaplan, D. L. *Nature* **2003**, *424* (6952), 1057–1061.
(8) Silver, F. H.; Freeman, J. W.; Seehra, G. P. *J. Biomech.* **2003**, *36* (10), 1529–1553.
(9) Baer, E.; Cassidy, J. J.; Hiltner, A. *Pure Appl. Chem.* **1991**, *63* (7), 961–973.
(10) Fratzl, P. *Curr. Opin. Colloid Interface Sci.* **2003**, *8* (1), 32–39.
(11) Wess, T. J. *Fibrous Proteins* **2005**, *70*, 341–374.
(12) Young, P. A.; Lovell, R. J. *Introduction to Polymers*; CRC Press: Boca Raton, FL, 1991; Vol. *2*.
(13) Ji, X. L.; Jing, J. K.; Jiang, W.; Jiang, B. Z. *Polym. Eng. Sci.* **2002**, *42* (5), 983–993.
(14) Hussain, F.; Hojjati, M.; Okamoto, M.; Gorga, R. E. *J. Compos. Mater.* **2006**, *40* (17), 1511–1575.
(15) Komarneni, S. *J. Mater. Chem.* **1992**, *2* (12), 1219–1230.
(16) Laine, R. M.; Choi, J. W.; Lee, I. *Adv. Mater.* **2001**, *13* (11), 800–803.
(17) Crosby, A. J.; Lee, J. Y. *Polym. Rev.* **2007**, *47* (2), 217–229.
(18) Jordan, J.; Jacob, K. I.; Tannenbaum, R.; Sharaf, M. A.; Jasiuk, I. *Mater. Sci. Eng., A* **2005**, *393* (1−2), 1–11.
(19) Manias, E. *Nature Mater.* **2007**, *6* (1), 9–11.
(20) Breuer, O.; Sundararaj, U. *Polym. Compos.* **2004**, *25* (6), 630–645.
(21) Huo, Q. S.; Margolese, D. I.; Ciesla, U.; Demuth, D. G.; Feng, P. Y.; Gier, T. E.; Sieger, P.; Firouzi, A.; Chmelka, B. F.; Schuth, F.; Stucky, G. D. *Chem. Mater.* **1994**, *6* (8), 1176–1191.
(22) Manias, E.; Touny, A.; Wu, L.; Strawhecker, K.; Lu, B.; Chung, T. C. *Chem. Mater.* **2001**, *13* (10), 3516–3523.
(23) Schmidt, G.; Malwitz, M. M. *Curr. Opin. Colloid Interface Sci.* **2003**, *8* (1), 103–108.
(24) Sanchez, C.; Lebeau, B.; Chaput, F.; Boilot, J. P. *Adv. Mater.* **2003**, *15* (23), 1969–1994.
(25) Beecroft, L. L.; Ober, C. K. *Chem. Mater.* **1997**, *9* (6), 1302–1317.
(26) Innocenzi, P.; Lebeau, B. *J. Mater. Chem.* **2005**, *15* (35−36), 3821–3831.
(27) Gangopadhyay, R.; De, A. *Chem. Mater.* **2000**, *12* (3), 608–622.
(28) Bauhofer, W.; Kovacs, J. Z. *Compos. Sci. Technol.* **2009**, *69* (10), 1486–1498.
(29) Grossiord, N.; Loos, J.; Regev, O.; Koning, C. E. *Chem. Mater.* **2006**, *18*, 1089–1099.
(30) Herring, A. M. *Polym. Rev.* **2006**, *46* (3), 245–296.
(31) Shokouhimehr, M.; Piao, Y. Z.; Kim, J.; Jang, Y. J.; Hyeon, T. *Angew. Chem., Int. Ed.* **2007**, *46*, 7039–7043.
(32) Zandi-zand, R.; Ershad-langroudi, A.; Rahimi, A. *Prog. Org. Coat.* **2005**, *53* (4), 286–291.
(33) Lau, K. T.; Hui, D. *Composites, Part B* **2002**, *33* (4), 263–277.
(34) Lin, Y.; Zhou, B.; Fernando, K. A. S.; Liu, P.; Allard, L. F.; Sun, Y. P. *Macromolecules* **2003**, *36* (19), 7199–7204.
(35) Samir, M.; Alloin, F.; Dufresne, A. *Biomacromolecules* **2005**, *6* (2), 612–626.
(36) Habibi, Y.; Lucia, L. A.; Rojas, O. J. *Chem. Rev.* **2010**, *110* (6), 3479–500.
(37) Orts, W. J.; Shey, J.; Imam, S. H.; Glenn, G. M.; Guttman, M. E.; Revol, J. F. *J. Polym. Environ.* **2005**, *13* (4), 301–306.
(38) Sturcova, A.; Davies, G. R.; Eichhorn, S. J. *Biomacromolecules* **2005**, *6* (2), 1055–1061.
(39) Habibi, Y.; Lucia, L. A.; Rojas, O. J. *Chem. Rev.* **2010**, *110* (6), 3479–3500.
(40) Shanmuganathan, K.; Capadona, J. R.; Rowan, S. J.; Weder, C. *Prog. Polym. Sci.* **2010**, *35* (1−2), 212–222.
(41) Eichhorn, S. J.; Baillie, C. A.; Zafeiropoulos, N.; Mwaikambo, L. Y.; Ansell, M. P.; Dufresne, A.; Entwistle, K. M.; Herrera-Franco, P. J.; Escamilla, G. C.; Groom, L.; Hughes, M.; Hill, C.; Rials, T. G.; Wild, P. M. *J. Mater. Sci.* **2001**, *36* (9), 2107–2131.
(42) Eichhorn, S. J.; Dufresne, A.; Aranguren, M.; Marcovich, N. E. Capadona, J. R.; Rowan, S. J.; Weder, C.; Thielemans, W.; Roman, M.; Renneckar, S.; Gindl, W.; Veigel, S.; Keckes, J.; Yano, H.; Abe, K.; Nogi, M.; Nakagaito, A. N.; Mangalam, A.; Simonsen, J.; Benight, A. S.; Bismarck, A.; Berglund, L. A.; Peijs, T. *J. Mater. Sci.* **2010**, *45* (1), 1–33.
(43) Yano, H.; Sugiyama, J.; Nakagaito, A. N.; Nogi, M.; Matsuura, T.; Hikita, M.; Handa, K. *Adv. Mater.* **2005**, *17* (2), 153–155.
(44) Tang, L. M.; Weder, C. *ACS Appl. Mater. Interfaces* **2010**, *2* (4), 1073–1080.
(45) Rusli, R.; Shanmuganathan, K.; Rowan, S. J.; Weder, C.; Eichhorn, S. J. *Biomacromolecules* **2010**, *11* (3), 762–768.
(46) Gierlinger, N.; Schwanninger, M.; Reinecke, A.; Burgert, I. *Biomacromolecules* **2006**, *7* (7), 2077–2081.
(47) Quero, F.; Nogi, M.; Yano, H.; Abdulsalami, K.; Holmes, S. M.; Sakakini, B. H.; Eichhorn, S. J. *ACS Appl. Mater. Interfaces* **2009**, *2* (1), 321–330.
(48) Gawryla, M. D.; van den Berg, O.; Weder, C.; Schiraldi, D. A. *J. Mater. Chem.* **2009**, *19* (15), 2118–2124.
(49) Sehaqui, H.; Salajkova, M.; Zhou, Q.; Berglund, L. A. *Soft Matter* **2010**, *6* (8), 1824–1832.
(50) Paakko, M.; Vapaavuori, J.; Silvennoinen, R.; Kosonen, H.; Ankerfors, M.; Lindstrom, T.; Berglund, L. A.; Ikkala, O. *Soft Matter* **2008**, *4* (12), 2492–2499.
(51) Svagan, A. J.; Samir, M.; Berglund, L. A. *Adv. Mater.* **2008**, *20* (7), 1263–1269.
(52) Capadona, J. R.; Shanmuganathan, K.; Tyler, D. J.; Rowan, S. J.; Weder, C. *Science* **2008**, *319* (5868), 1370–1374.
(53) Shanmuganathan, K.; Capadona, J. R.; Rowan, S. J.; Weder, C. *J. Mater. Chem.* **2010**, *20* (1), 180–186.
(54) Whitesides, G. M.; Grzybowski, B. *Science* **2002**, *295* (5564), 2418–2421.
(55) Alivisatos, A. P.; Barbara, P. F.; Castleman, A. W.; Chang, J.; Dixon, D. A.; Klein, M. L.; McLendon, G. L.; Miller, J. S.; Ratner, M. A.; Rossky, P. J.; Stupp, S. I.; Thompson, M. E. *Adv. Mater.* **1998**, *10* (16), 1297–1336.
(56) Palmer, L. C.; Stupp, S. I. *Acc. Chem. Res.* **2008**, *41* (12), 1674–1684.
(57) Abdallah, D. J.; Weiss, R. G. *Adv. Mater.* **2000**, *12* (17), 1237–1247.
(58) Sofos, M.; Goldberger, J.; Stone, D. A.; Allen, J. E.; Ma, Q.; Herman, D. J.; Tsai, W. W.; Lauhon, L. J.; Stupp, S. I. *Nature Mater.* **2009**, *8* (1), 68–75.
(59) Hasegawa, M.; Iyoda, M. *Chem. Soc. Rev.* **2010**, *39* (7), 2420–2427.
(60) Schenning, A.; Meijer, E. W. *Chem. Commun.* **2005**, *26*, 3245–3258.
(61) Stone, D. A.; Hsu, L.; Stupp, S. I. *Soft Matter* **2009**, *5* (10), 1990–1993.
(62) Ulijn, R. V.; Smith, A. M. *Chem. Soc. Rev.* **2008**, *37* (4), 664–675.
(63) Silva, G. A.; Czeisler, C.; Niece, K. L.; Beniash, E.; Harrington, D. A.; Kessler, J. A.; Stupp, S. I. *Science* **2004**, *303* (5662), 1352–1355.
(64) Feng, Y.; Jin, X.; Hay, J. N. *J. Appl. Polym. Sci.* **1998**, *69* (10), 2089–2095.
(65) Shepard, T. A.; Delsorbo, C. R.; Louth, R. M.; Walborn, J. L.; Norman, D. A.; Harvey, N. G.; Spontak, R. J. *J. Polym. Sci., Part B: Polym. Phys.* **1997**, *35* (16), 2617–2628.
(66) Smith, T. L.; Masilamani, D.; Bui, L. K.; Khanna, Y. P.; Bray, R. G.; Hammond, W. B.; Curran, S.; Belles, J. J.; Bindercastelli, S. *Macromolecules* **1994**, *27* (12), 3147–3155.
(67) Wilder, E. A.; Hall, C. K.; Khan, S. A.; Spontak, R. J. *Langmuir* **2003**, *19* (15), 6004–6013.
(68) Smith, J. M.; Katsoulis, D. E. *J. Mater. Chem.* **1995**, *5* (11), 1899–1903.
(69) Zubarev, E. R.; Pralle, M. U.; Sone, E. D.; Stupp, S. I. *J. Am. Chem. Soc.* **2001**, *123* (17), 4105–4106.
(70) Zubarev, E. R.; Sone, E. D.; Stupp, S. I. *Chem.—Eur. J.* **2006**, *12* (28), 7313–7327.
(71) Zubarev, E. R.; Pralle, M. U.; Sone, E. D.; Stupp, S. I. *Adv. Mater.* **2002**, *14* (3), 198–203.
(72) Stendahl, J. C.; Li, L. M.; Zubarev, E. R.; Chen, Y. R.; Stupp, S. I. *Adv. Mater.* **2002**, *14*, 1540–1543.
(73) Stendahl, J. C.; Zubarev, E. R.; Arnold, M. S.; Hersam, M. C.; Sue, H. J.; Stupp, S. I. *Adv. Funct. Mater.* **2005**, *15* (3), 487–493.
(74) Isare, B.; Petit, L.; Bugnet, E.; Vincent, R.; Lapalu, L.; Sautet, P.; Bouteiller, L. *Langmuir* **2009**, *25* (15), 8400–8403.
(75) Petit, L.; Lapalu, L.; Sautet, P. *J. Phys. Chem. C* **2009**, *113* (40), 17566–17571.
(76) Korley, L. T. J.; Liff, S. M.; Kumar, N.; McKinley, G. H.; Hammond, P. T. *Macromolecules* **2006**, *39* (20), 7030–7036.
(77) Wisse, E.; Govaert, L. E.; Meijer, H. E. H.; Meijer, E. W. *Macromolecules* **2006**, *39* (21), 7425–7432.
(78) Wisse, E.; Spiering, A. J. H.; Pfeifer, F.; Portale, G.; Siesler, H. W.; Meijer, E. W. *Macromolecules* **2009**, *42* (2), 524–530.
(79) Botterhuis, N. E.; Karthikeyan, S.; Veldman, D.; Meskers, S. C. J.; Sijbesma, R. P. *Chem. Commun.* **2008**, *33*, 3915–3917.
(80) Formalas, A. Process and Apparatus for Preparing Artificial Threads. U.S. Patent 1,975,504, 1934.
(81) Li, D.; Xia, Y. N. *Adv. Mater.* **2004**, *16* (14), 1151–1170.
(82) Li, W. J.; Laurencin, C. T.; Caterson, E. J.; Tuan, R. S.; Ko, F. K. *J. Biomed. Mater. Res.* **2002**, *60* (4), 613–621.
(83) Matthews, J. A.; Wnek, G. E.; Simpson, D. G.; Bowlin, G. L. *Biomacromolecules* **2002**, *3* (2), 232–238.

(84) Reneker, D. H.; Chun, I. *Nanotechnology* **1996**, *7* (3), 216 223.
(85) Deitzel, J. M.; Kleinmeyer, J.; Harris, D.; Tan, N. C. B. *Polymer* **2001**, *42* (1), 261–272.
(86) Huang, Z. M.; Zhang, Y. Z.; Kotaki, M.; Ramakrishna, S. *Compos. Sci. Technol.* **2003**, *63* (15), 2223–2253.
(87) Bergshoef, M. M.; Vancso, G. J. *Adv. Mater.* **1999**, *11* (16), 1362–1365.
(88) Kim, J. S.; Reneker, D. H. *Polym. Compos.* **1999**, *20* (1), 124–131.
(89) Tang, C. Y.; Liu, H. Q. *Composites, Part A* **2008**, *39* (10), 1638–1643.
(90) Luo, X. F.; Mather, P. T. *Macromolecules* **2009**, *42* (19), 7251–7253.